# Measurements on Subscale Y-Ba-Cu-O Racetrack Coils at 77 K and Self-Field

X. Wang, S. Caspi, D. W. Cheng, D. R. Dietderich, H. Felice, P. Ferracin,
A. Godeke, J. M. Joseph, J. Lizarazo, S. O. Prestemon and G. Sabbi

***Abstract*—$YBa_2Cu_3O_{7-\delta}$ (YBCO) tapes carry significant amount of current at fields beyond the limit of Nb-based conductors. This makes the YBCO tapes a possible conductor candidate for insert magnets to increase the bore field of $Nb_3Sn$ high-field dipoles. As an initial step of the YBCO insert technology development, two subscale racetrack coils were wound using Kapton-insulated commercial YBCO tapes. Both coils had two layers; one had 3 turns in each layer and the other 10 turns. The coils were supported by G10 side rails and waxed strips and not impregnated. The critical current of the coils was measured at 77 K and self-field. A 2D model considering the magnetic-field dependence of the critical current was used to estimate the expected critical current. The measured results show that both coils reached 80%–95% of the expected values, indicating the feasibility of the design concept and fabrication process.**

***Index Terms*—Insert magnets, racetrack coils, Y-Ba-Cu-O coated conductors.**

## I. Introduction

HIGHER magnetic fields are of critical interest for high-energy physics [1], [2] and numerous other scientific research areas [3]. In 2004, a peak bore field of 16 T was reached in a $Nb_3Sn$ dipole magnet at 4.5 K [4]. The magnetic-field dependence of the critical current density ($J_c(H)$) of $Bi_2Sr_2CaCu_2O_x$ (Bi-2212) and $YBa_2Cu_3O_{7-\delta}$ (YBCO) conductors surpasses that of $Nb_3Sn$ for fields above 18–22 T [3]. This motivates the application of these two conductors as insert elements in combination with existing $Nb_3Sn$ coils to achieve fields higher than 20 T for accelerator magnets [5], [6].

The performance of YBCO coated conductors has steadily improved in recent years, primarily driven by potential utility applications operating at 77 K. Significant progress has also been made in high-field magnet applications leveraging the higher critical currents ($I_c$) that are becoming available. For example, a coil with six double pancakes fabricated at SuperPower Inc. (SPI) generated 7.8 T in a background field of 19 T, reaching a total field of 26.8 T at 4.2 K [7]. More recently, an YBCO insert coil, composed of 380 turns, insulated with varnish but without impregnation, generated 2.8 T in a background field of 31 T, setting another record of 33.8 T at 4.2 K [8], [9].

Manuscript received December 9, 2009. This work was supported by the Director, Office of Science, High Energy Physics, U.S. Department of Energy under contract No. DE-AC02-05CH11231.

The authors are with Lawrence Berkeley National Laboratory, Berkeley, CA, 94720 USA (e-mail: {XRWang, S_Caspi, DWCheng, DRDietderich, HFelice, PFerracin, AGodeke, JMJoseph, JLizarazo, SOPrestemon, GLSabbi}@lbl.gov).

At Lawrence Berkeley National Laboratory (LBNL), high-field magnet inserts based on both Bi-2212 Rutherford cables [5], [10], [11] and YBCO tape conductors are under investigation through a subscale coil program similar to the one developed for $Nb_3Sn$ [12]–[14]. In this article, we summarize the results of recent efforts on YBCO coil technology development at LBNL.

## II. YBCO Tape Conductor

The conductor (SCS4050) is manufactured by SPI [15]. The bare tape is 4.0 mm wide and 0.095 mm thick. The conductor has a 50 $\mu$m thick Hastelloy C-276 substrate. The tape is insulated by the vendor using 50 $\mu$m thick Kapton tapes with 30% overlap. The critical current ($I_c$) was measured every 5 m by the vendor. The minimum $I_c$ of a 100 m long conductor is 154 A at 77 K and self-field. The $I_c$ profile along 100 m has a standard deviation of 6.26%; the $n$-value is around 32.

Several 10 cm long samples, cut from the same spool as the conductors used to wind the coils were used to characterize the conductor $I_c$ at 77 K and self-field. The short sample $I_c$ was consistent with those reported by the vendor. No reduction in $I_c$ was found for bending diameters larger than 9 mm, when the samples were bent in the easy way with the YBCO on the out/inside [16].

## III. Coil Fabrication and Test

### A. Coil Fabrication

Two double-layer racetrack coils, YC01 and YC02, were wound on stainless steel 304 pole-islands following the subscale coil concept [5], [10], [12]. The pole-islands are 190 mm long, 37 mm wide and 9 mm thick. Coil YC01 has $2 \times 3$ turns and coil YC02 has $2 \times 10$ turns. To test the first steps of the coil fabrication process, e.g., winding and soldering, no vacuum impregnation was performed. Both coils were constrained only by G10 side bars (2 mm thick) and were wrapped with waxed string in the straight section (Fig. 1). The end support structures, e.g., horseshoe and endshoe commonly used for subscale coils [12], were not implemented. This configuration allowed for iterative $I_c$ measurements in different segments.

Typical tension used during the winding is 6 N, corresponding to a tensile stress of $\sim 30$ MPa in the Hastelloy substrate, well below its yield limit of 455 MPa 295 K [17]. Given the Hastelloy modulus of 195 GPa at room temperature [17], 30 MPa yields a tensile strain of 0.02%, which is below the critical applied axial strain in the specification [18] as well as other published results [19], [20]. In addition, the YBCO

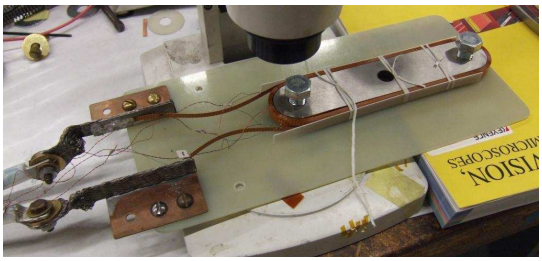

Fig. 1. Coil YC02 as mounted on the coil holder before the test. Layer A was the top layer and layer B was facing the G10 board.

side of the conductor faces the pole-island during the winding so that the YBCO layer is under compression to cancel at least part of the hoop stress when the coil is energized. The conductor is continuously wound around the pole-island from one layer to the other to form the transition between layers (ramp). It took about 2.6 m to wind coil YC01 and 8.5 m for coil YC02.

At each voltage tap location, a pair of twisted Cu instrumentation wires (AWG 32 and Polymide insulation) is soldered (Sn96/Ag4 solder) to the conductor edge with a contact length $\lesssim 1.5$ mm. To minimize the possible conductor $I_c$ degradation due to soldering, only two or three voltage taps are installed before the test. Additional voltage taps are installed during subsequent thermal cycles. No obvious $I_c$ change is observed with the addition of more voltage taps.

### *B. Coil Measurement*

The pole-island is bolted to a G10 board (Fig. 1). Two oxygen-free high-conductivity Cu sheets with a "L"-shaped cross section are bolted at one end of the board to serve as the current leads. The two lead conductors from the coil are soldered to the Cu sheets with a contact length of $\sim 25$ mm. The lead conductors are slightly bent to minimize strain due to thermal contraction during cooldown. The power cables are bolted to the Cu sheets for easy attachment. During the test, the coil assembly is submerged in liquid nitrogen at 77 K.

The coil measurement consists primarily of $I_c$ measurements of different coil segments. To determine $I_c$ using an electric-field criterion, the segment lengths are determined at room temperature by measuring their resistances. During excitation, the segment and shunt voltages are measured by digital multi-meters (DMMs, HP3458A and HP3457A). The DMMs are triggered to take measurements simultaneously. Typical sampling rate is 1 Hz, which is sufficient due to the slow quench process at 77 K and in low field. Note that this is three orders lower than the typical sampling rate of 5 kHz for capturing the quench propagation in $Nb_3Sn$ magnets used at LBNL [21]. A power supply (EMS, 7.5 V, 1 kA) is controlled to provide the desired current. All instruments are controlled by a PC via an IEEE-488 bus.

The current is ramped in a step-and-hold manner to minimize the inductive voltage. Several voltage measurements are averaged at the same current level. The hysteresis of the $V(I)$ curve was checked by ramping the current down when the coil voltage was above $\sim 10$ mV. The curve retraced itself and no excessive heating was found. Coil YC02 has an inductance of 100 $\mu$H, yielding only 2 J of stored energy at a transport current of 200 A. Thus, no specific quench protection scheme is used in the test.

## IV. Field Dependence of Critical Current at 77 K

The $I_c$ of an YBCO tape strongly depends on the magnetic field direction, and is especially sensitive to the component perpendicular to the tape surface at 77 K due to the anisotropy associated with the layered structure of YBCO. Hence, it is necessary to consider the magnetic-field dependence of the critical current when determining the expected coil $I_c$. Here a 2D model based on the approach proposed by Babaei Brojeny and Clem [22] is used to estimate the self-field $I_c$ of a racetrack coil with the same cross section as YC01/YC02 but with an infinitely long straight section (Fig. 2). The current density distribution ($J$) in each turn of the coil that is self-consistent with the resulting field distribution is calculated using the 2D model.

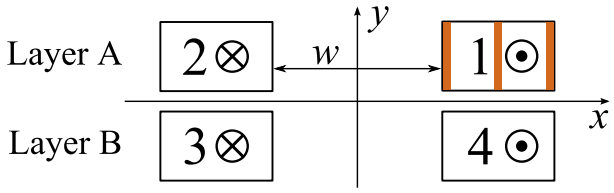


Fig. 2. Cross section of a racetrack coil with an infinitely-long straight section (not to scale). Layer A: coil pack 1 and 2; layer B: coil pack 3 and 4. Three turns are shown in coil pack 1. $w$ is the pole-island width.

Define $J_n(x, y)$ as the current density in each turn of the coil. The subscript $n$ is the number of the coil pack (Fig. 2). Due to the symmetry, $J_1(x, y) = -J_2(-x, y) = -J_3(-x, -y) = J_4(x, -y)$. Each turn is discretized in a 1D grid along the $y$ direction because of the high aspect ratio of the conductor.

Only the $B_x$ (perpendicular to the tape surface) dependence of the conductor $I_c$ at 77 K is considered for simplicity. The Kim model [22] is used to describe the field dependence, i.e., $J_c(B_x) = J_0/(1 + |B_x|/B_0)$, where $J_c = I_c/A$ and $A$ is the area of the YBCO layer ($0.004$ mm$^2$). Fitting the Kim model to the $I_c(B_x)$ measured by SPI [23] using a least-squares method yields $J_0 = 0.05$ MA/mm$^2$ and $B_0 = 115.04$ mT. The range of $B_x$ used for the fit was 0.1 T - 2.5 T. Given a typical short sample $I_c$ of 180 A at 77 K self-field, we find good agreement between the calculated and measured short sample $I_c(B_x)$ [23].

## V. Results

### *A. Expected Coil $I_c$*

The $I_c$ of each turn is given by $I = \int J(y)\mathrm{d}y$, where $J(y)$ is the current density distribution in each turn given by the 2D model. As shown in Fig. 3 insert, $J(y)$ is not uniform in the conductor because of the field distribution; $J_1|_{y\approx 0.5\text{ mm}} = J_0$ indicates that $B_x = 0$ close to the mid-plane ($x$-axis, Fig. 2). This is mainly due to the field contributed from coil pack 4. Fig. 3 shows the $I_c$ for each turn in coil pack 1, normalized

to the short sample $I_c$ (180 A) at 77 K and self-field, in $2 \times 3$-turn and $2 \times 10$-turn coils. The concave $I_c$-turn distribution is consistent with the stronger $B_x$ in the middle turns. The symmetric distributions indicate a small effect from coil packs 2 and 3 for a pole-island width of 37 mm.

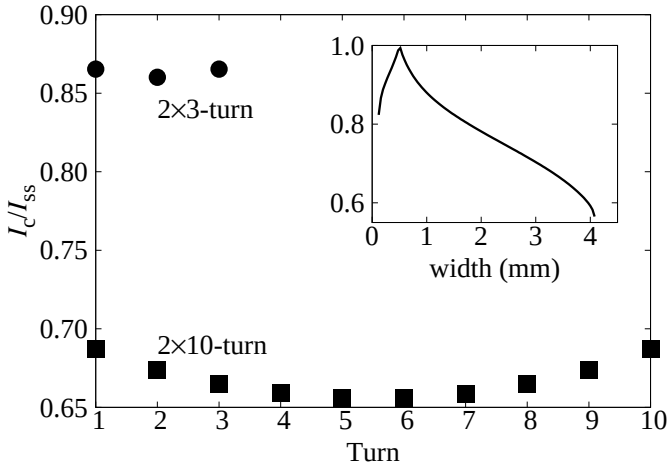


Fig. 3. $I_c$ of each turn in coil pack 1, normalized to the short sample $I_c$, for a $2 \times 3$-turn (solid circles) and a $2 \times 10$-turn coil (squares) at 77 K and self-field. The insert shows the non-uniform $J_1(y)/J_0$ of turn 2 in a $2 \times 3$-turn coil.

The coil $I_c$ is defined as the lowest $I_c$ of all the turns. Thus we have $I_c = 154$ A for a $2 \times 3$-turn coil and $I_c = 118$ A for a $2 \times 10$-turn coil. Both coils have the same cross-section geometry as YC01 and YC02, respectively, but with infinitely-long straight sections.

### *B. YC01 – The $2 \times 3$-Turn Coil*

Three voltage tap pairs were soldered to coil YC01 to measure three segments: the whole coil, layer A and layer B. The ramp was included in the voltage tap pair for layer B. Fig. 4 shows the measured electric field ($E$) versus current of three segments in a log-log scale.

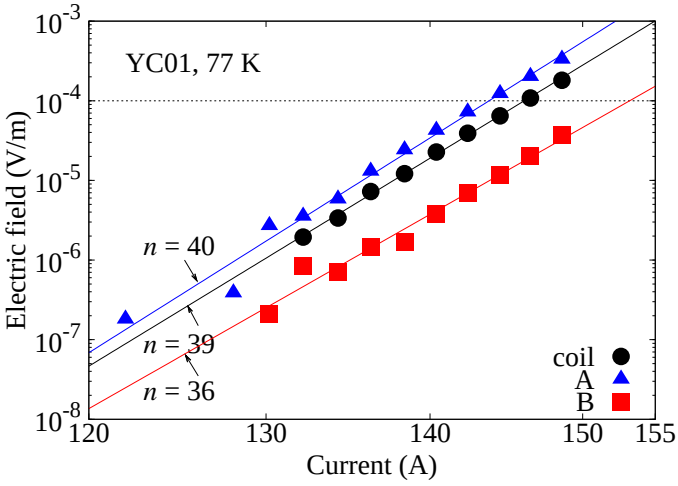


Fig. 4. $E(I)$ of the three segments in YC01 measured at 77 K (log-log scale).

Using an electric-field criterion $E_c = 10^{-4}$ V/m, one has $I_{c,coil} = 146$ A, $n = 39$; $I_{c,A} = 144$ A, $n = 40$; and $I_{c,B} = 153$ A, $n = 36$. Both layers have comparable $I_c$ values.

### *C. YC02 – The $2 \times 10$-Turn Coil*

Similar to YC01, coil YC02 had three voltage taps in the initial tests and the ramp section was included in the layer B voltage tap pair. The whole coil voltage of YC02 consists primarily of layer B (Fig. 5): $I_{c,coil} = 107$ A, $n = 33$ and $I_{c,B} = 104$ A, $n = 31$ using $E_c = 10^{-4}$ V/m. $I_{c,A}$ is estimated to be at least 15 A higher than $I_{c,B}$.

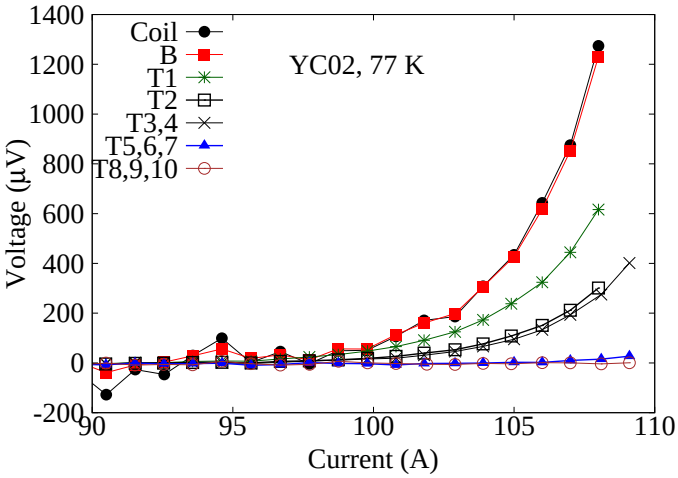


Fig. 5. $V(I)$ of turns in layer B of YC02 measured at 77 K.

Voltage taps were added in layer B such that layer B = 1 + 2 + (3, 4) + (5, 6, 7) + (8, 9, 10), expressed in terms of turn number. Turns grouped by parentheses were measured as one segment. The pole turn (turn 1) has the highest voltage for the same current, followed by turn 2 and turns (3,4) (Fig. 5). At a peak current of 109 A, the voltage of turns (5,6,7) increases only to 27 $\mu$V. No voltage rise is observed in turns (8,9,10), indicating that its $I_c > 109$ A. The corresponding $E(I)$ curves on a double log scale are shown in Fig. 6.

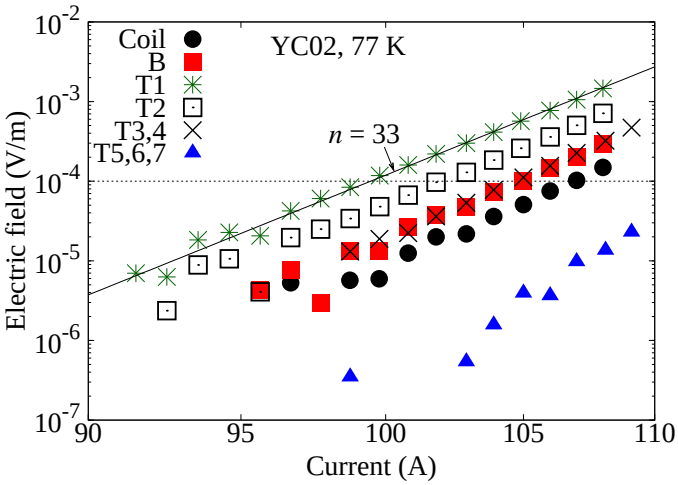


Fig. 6. $E(I)$ of the turns in layer B of YC02 measured at 77 K (log-log scale).

The $I_c$ values of the outer turns are higher than the inner turns; $n \gtrsim 30$ for all the turns. The coil and layer B show

similar voltages; turn 2 and turn (3,4) have similar voltages (Fig. 5). Their $I_c$ values, as determined by the same $E_c$ criterion, however, are not equal (Fig. 6).

## VI. Discussion

The measured $I_c$ of the whole coil or a segment of the coil is used to assess the coil fabrication technology. Magnetic field and mechanical issues are two major factors influencing $I_c$ in a coil. Magnetic effects result from the field dependence of the conductor $I_c$. Mechanical issues are mainly strain-induced $I_c$ reduction that could be 1) pure mechanical, e.g., conductor handling, coil winding and pre-load; 2) coupled with thermal stress/strain, e.g., in a quench; and 3) coupled with magnetic field and current distribution, e.g., Lorentz load and hoop stress. The primary goals of the coil technology development are 1) to separate the $I_c$ reduction due to the magnetic-field effect and that due to the mechanical effect [24] and 2) to identify, understand, and minimize the $I_c$ reduction resulting from the coil fabrication process.

The 2D model (section IV) establishes a baseline $I_c$ considering only the field-induced $I_c$ reduction. Both YC01 and YC02 had good performance, as the measured coil $I_c$ reached $\geq 90\%$ of the expected values (Table I), indicating the preliminary coil fabrication techniques are acceptable.

TABLE I
Measured and expected $I_C$ for YC01 and YC02.

| | YC01 | YC02 | | |
|---|---|---|---|---|
| Segment | Coil | Coil | Turn 1 | Turn 2 |
| $a$. Measured $I_c$ (A) | 146 | 107 | 100 | 102 |
| $b$. Expected $I_c$ (A) | 154 | 118 | 124 | 121 |
| $a/b$ | 95% | 91% | 81% | 84% |

There may be two reasons why the coils did not reach their full potential, in addition to the possible non-uniform $I_c$ as a function of conductor length. The actual coil and turn $I_c$ could be lower than the calculated values shown in Table I due to 1) the 2D model neglects slightly enhanced end fields for a racetrack coil and 2) the $B_y$-dependence of $I_c$ ($B_y \parallel$ tape surface) is not considered. The other reason is that the strain-dependence of the conductor $I_c$ is not considered in the 2D electromagnetic model [24]. For example, the bending strain of the pole turn wound around the curvature of the pole-island (radius of 19 mm) was estimated to be $\sim -0.13\%$ (compressive) that may account for a reversible $2\%$ $I_c$ reduction from a straight sample [25]. The measured turn and layer $I_c$ of coil YC02 suggest strain-induced $I_c$ reduction might occur. First, both layers should have similar $I_c$ if only magnetic-field effects were in play. Second, inner turns should have higher $I_c$ as predicted by the 2D model (Fig. 3) while the measured results show they were the lowest (Figs. 5 and 6, Table I).

The ramp, physically next to the pole turn, may be another segment requiring more investigation. The strain state of the ramp is not easily accessible as it experiences both easy- and hard-way bend that may reduce the local $I_c$ [25]. The measurement of layer B included the ramp in both coils. In coil YC01, layer B had the highest $I_c$ while in coil YC02, layer B had the lowest $I_c$. For coil YC01, the ramp was more gradual, starting from the far end of the straight segment while in coil YC02, the ramp was restricted to the near ends of the straight segments in both layers. A long ramp is favorable in terms of coil winding as it makes the hard-way bend transition in a more continuous and gentle way.

On the other hand, some ambiguity on the $I_c$ determination arose from the $E_c$ criterion. Here $E = V/L$; $V$ and $L$ are the segment voltage and length, respectively. The criterion is generally used for short samples where $I_c$ is usually uniform. When the conductor length increases (e.g., in a coil), however, $I_c$ fluctuation could occur along the length due to the field/strain effects as mentioned above. In this case, $I_c$ based on criteria involving averaging over $L$ may be ambiguous as its value depends on $L$ while the actual $V(I)$ is fixed. For example, even though the coil and layer B have similar $V(I)$ curves in YC02 (Fig. 5), $I_{c,coil} > I_{c,B}$ since $L_{coil} \approx 2L_B$ (Fig. 6). To reduce the effect due to averaging over the length, one may define a quench current ($I_q$) based on a certain $V$. Thus, segments with similar voltages always have similar $I_q$ regardless of their lengths. The voltage level from which $I_q$ is defined could be determined based on the voltage threshold to be used in a quench detection system.

## VII. Summary and Next Steps

Two YBCO subscale racetrack coils ($2 \times 3$-turn and $2 \times 10$-turn) were fabricated and tested at 77 K. The commercial conductor is Kapton-insulated and has a typical $I_c$ of 180 A and $n$ value of 32 at 77 K, self-field. The coils are supported by G10 side rails and are not vacuum impregnated. Coil $I_c$ is measured to assess the fabrication techniques. The expected coil $I_c$ is calculated using a 2D model considering the magnetic-field effect. Both coils reached 80%–95% of the expected $I_c$, indicating the general feasibility of the coil fabrication process.

Magnetic and mechanical effects will be studied in more details. Compatibility with vacuum impregnation procedures will also be investigated. More coils will be wound and measured at 4.2 K. Successful coils will be tested as inserts in existing high-field $Nb_3Sn$ dipoles.

## Acknowledgment

The authors thank P. Bish, R. Hannaford, H. Higley, C. Kozy, N. Liggins, J. Swanson for their technical expertise, and B. Bingham, B. Lilley, D. Tam and F. Trillaud for their help with the test.

## References

[1] S. Gourlay, "Challenges and prospects for the large-scale application of superconductivity," *IEEE Trans. Appl. Supercond.*, vol. 18, no. 3, pp. 1671–1680, 2008.

[2] A. Devred, S. Gourlay, and A. Yamamoto, "Future accelerator magnet needs," *IEEE Trans. Appl. Supercond.*, vol. 15, no. 2, pp. 1192–1199, June 2005.

[3] J. Schwartz, T. Effio, X. Liu *et al.*, "High field superconducting magnets via high temperature superconductors," *IEEE Trans. Appl. Supercond.*, vol. 18, no. 2, pp. 70–81, 2008.

[4] A. F. Lietzke, S. Bartlett, P. Bish *et al.*, "Test results for HD1, a 16 Tesla $Nb_3Sn$ dipole magnet," *IEEE Trans. Appl. Supercond.*, vol. 14, no. 2, pp. 345–348, 2004.

[5] A. Godeke, D. Cheng, D. R. Dietderich *et al.*, "Development of wind-and-react Bi-2212 accelerator magnet technology," *IEEE Trans. Appl. Supercond.*, vol. 18, pp. 516–519, 2008.

[6] G. de Rijk, "New European accelerator project EuCARD: work package on high field magnets," 2009, IEEE/CSC & ESAS European Superconductivity News Forum, No.8, http://www.ewh.ieee.org/tc/csc/europe/newsforum/pdf/RN-10.pdf.

[7] D. W. Hazelton, V. Selvamanickam, J. M. Duval *et al.*, "Recent developments in 2G HTS coil technology," *IEEE Trans. Appl. Supercond.*, vol. 19, pp. 2218–2222, Jun. 2009.

[8] W. Markiewicz, K. Pickard, H. Weijers *et al.*, "33.8 Tesla with a $YBa_2Cu_3O_{7-X}$ superconducting test coil," National High Magnetic Field Laboratory, Tech. Rep., 2008.

[9] H. Weijers, W. Markiewicz, K. Pickard *et al.*, "Tests of HTS insert coils above 30 T," presented at International Symposium on Superconductivity (ISS-2008), Tsukuba, Japan, October 27-29 (2008).

[10] A. Godeke, D. Cheng, D. R. Dietderich *et al.*, "Limits of NbTi and $Nb_3Sn$, and development of W&R Bi-2212 high field accelerator magnets," *IEEE Trans. Appl. Supercond.*, vol. 17, no. 2, pp. 1149–1152, 2007.

[11] A. Godeke, D. W. Cheng, D. R. Dietderich *et al.*, "Progress in wind-and-react Bi-2212 accelerator magnet technology," *IEEE Trans. Appl. Supercond.*, vol. 19, pp. 2228–2231, Jun. 2009.

[12] R. Hafalia, S. Caspi, L. Chiesa *et al.*, "An approach for faster high field magnet technology development," *IEEE Trans. Appl. Supercond.*, vol. 13, no. 2, pp. 1258–1261, 2003.

[13] P. Ferracin, G. Ambrosio, E. Barzi *et al.*, "Assembly and tests of SQ02, a $Nb_3Sn$ racetrack quadrupole magnet for LARP," *IEEE Trans. Appl. Supercond.*, vol. 17, no. 2, pp. 1019–1022, 2007.

[14] H. Felice, S. Caspi, D. R. Dietderich *et al.*, "Design and test of a $Nb_3Sn$ subscale dipole magnet for training studies," *IEEE Trans. Appl. Supercond.*, vol. 17, no. 2, pp. 1144–1148, 2007.

[15] V. Selvamanickam, Y. Chen, X. Xiong *et al.*, "Progress in second-generation HTS wire development and manufacturing," *Physica C*, vol. 468, no. 15–20, pp. 1504–1509, 2008.

[16] B. C. Lilley, H. Felice, and X. Wang, "Determination of the critical bending diameter for $YBa_2Cu_3O_{7-\delta}$ coated conductors," Lawrence Berkeley National Laboratory, Tech. Rep., August 2009, Science Undergraduate Laboratory Intership, Office of Science, Department of Energy.

[17] C. Clickner, J. Ekin, N. Cheggour *et al.*, "Mechanical properties of pure Ni and Ni-alloy substrate materials for Y-Ba-Cu-O coated superconductors," *Cryogenics*, vol. 46, pp. 432–438, 2006.

[18] SuperPower Inc., "2G HTS wire for coil applications," August 2008.

[19] N. Cheggour, J. W. Ekin, C. L. H. Thieme *et al.*, "Reversible axial-strain effect in Y-Ba-Cu-O coated conductors," *Superconductor Science and Technology*, vol. 18, pp. S319–S324, 2005.

[20] D. C. van der Laan and J. W. Ekin, "Large intrinsic effect of axial strain on the critical current of high-temperature superconductors for electric power applications," *Applied Physics Letter*, vol. 90, no. 5, p. 052506, 2007.

[21] P. Ferracin, B. Bingham, S. Caspi *et al.*, "Assembly and test of HD2, a 36 mm bore high field $Nb_3Sn$ dipole magnet," *IEEE Trans. Appl. Supercond.*, vol. 19, no. 3, pp. 1240–1243, 2009.

[22] A. A. Babaei Brojeny and J. R. Clem, "Self-field effects upon the critical current density of flat superconducting strips," *Superconductor Science and Technology*, vol. 18, pp. 888–895, 2005.

[23] D. W. Hazelton, "Continued developments in high magnetic fields enabled by second-generation high-temperature superconductors," Presented at 2009 Magnetics Conference, Chicago, IL April 15-16, 2009.

[24] P. Fabbricatore, C. Priano, M. P. Testa *et al.*, "Field distribution effect on the performances of coils wound with Ag/Bi-2223 tape," *Superconductor Science and Technology*, vol. 11, pp. 304–310, 1998.

[25] D. C. van der Laan and J. W. Ekin, "Dependence of the critical current of $YBa_2Cu_3O_{7-\delta}$ coated conductors on in-plane bending," *Superconductor Science and Technology*, vol. 21, no. 11, p. 115002, Nov. 2008.